

Research Article

Wind Power Assessment Based on a WRF Wind Simulation with Developed Power Curve Modeling Methods

Zhenhai Guo and Xia Xiao

*State Key Laboratory of Numerical Modeling for Atmospheric Sciences and Geophysical Fluid Dynamics,
Institute of Atmospheric Physics, Chinese Academy of Sciences, Beijing 100029, China*

Correspondence should be addressed to Xia Xiao; xiaoxia@lasg.iap.ac.cn

Received 14 April 2014; Accepted 16 May 2014; Published 21 July 2014

Academic Editor: Jianzhou Wang

Copyright © 2014 Z. Guo and X. Xiao. This is an open access article distributed under the Creative Commons Attribution License, which permits unrestricted use, distribution, and reproduction in any medium, provided the original work is properly cited.

The accurate assessment of wind power potential requires not only the detailed knowledge of the local wind resource but also an equivalent power curve with good effect for a local wind farm. Although the probability distribution functions (pdfs) of the wind speed are commonly used, their seemingly good performance for distribution may not always translate into an accurate assessment of power generation. This paper contributes to the development of wind power assessment based on the wind speed simulation of weather research and forecasting (WRF) and two improved power curve modeling methods. These approaches are improvements on the power curve modeling that is originally fitted by the single layer feed-forward neural network (SLFN) in this paper; in addition, a data quality check and outlier detection technique and the directional curve modeling method are adopted to effectively enhance the original model performance. The proposed two methods, named WRF-SLFN-OD and WRF-SLFN-WD, are able to avoid the interference from abnormal output and the directional effect of local wind speed during the power curve modeling process. The data examined are from three stations in northern China; the simulation indicates that the two developed methods have strong abilities to provide a more accurate assessment of the wind power potential compared with the original methods.

1. Introduction

1.1. Wind Energy and the Related Power Potential Assessment.

Currently, for both developed and developing countries, the heavy dependence on fossil fuels has caused serious environmental problems, such as atmospheric pollution and soil and water contaminations. The threat of global warming and the rapid depletion of nonrenewable energy resources are now driving one of the greatest transitions in the energy field in the history of human civilization. Consequently, renewable energy is considered to be the most promising alternative energy resource because it plays a significant role in securing the long-term sustainable energy supply and reducing global greenhouse gases emissions [1]. As the most active approach, wind power demonstrates its strong benefits and good prospects; its utilization is increasing around the world at an accelerating pace, and a large number of wind farms have been built for power generation. In fact, because wind is highly uncertain in both space and time, the main

obstacle for wind industry development is the variability of the output power, which seriously limits wind power penetration and threatens grid security. As a result, the development of new wind projects persists in being hampered by the lack of reliable and accurate wind resource data in many regions of the world. Such data are needed to enable governments, private developers, and others to determine the priority that should be given to wind energy utilization and to identify the potential areas that might be suitable for development [2, 3].

Wind energy is characterized by strong instability and intermittency, mainly as a result of the atmospheric circulation, making it difficult to estimate the generated power that is needed to be injected into the grid and also causing difficulties for energy transportation [4]. To build up wind farms, it is essential to perform an accurate assessment of the wind energy potential at promising sites [5] because the availability of wind resources varies with location. Therefore, an accurate wind power assessment is an important and

critical factor to be well understood for harnessing the wind-generated power output. Not only is it an essential part of the development of wind power utilization but also it provides the investors with the necessary confidence in financial feasibility and mitigating risks [6]. In reality, the development and construction of a wind farm is a process of stage extension; the wind resource assessment is a crucial step both in the preevaluation for the site selection and in planning additional wind energy projects; detailed knowledge of the wind resource at a local site is needed to estimate the performance of a wind energy project. In general, there are two categories of power assessment methods; the first is the estimation directly based on the power records, mainly using prediction techniques, and the second is the evaluation of wind speeds according to the transition of power curves. Considering the stage-construction project of a wind farm, power assessment is crucial to determine the future investment behavior for both the development scale and the operation mode of a wind farm. In this case, future power estimations cannot be directly obtained from the historical power records, mainly due to the change of installation. Thus, the feasible method is to model the transition relationship from wind speed to turbine power output.

1.2. Assessment of Wind Power Potential: Existing Works. Researchers have exerted great effort toward the wind power assessment of a local site, which can be categorized into two major groups when considering the application of the stage-construction wind farms [7]. One group is the wind power assessment based on historical records, which mainly combines the wind speed distribution and the WT power curve [8]; the other group is the prediction of the future power output through the historical data using statistical or physical models [9].

Although the power output from wind turbines (WTs) varies with the cube of the wind speed at the hub height, the wind speed is not constant with time, which makes it difficult to evaluate the accurate power output. To effectively evaluate the wind power available for a particular site, the statistical analysis, which concerns the use of various probability density functions (pdfs) to describe wind speed frequency distributions, is generally used. The pdf of wind speed distribution indicates how often wind of different speeds will occur at a local site with a certain average wind speed; there are different distribution functions for determining the wind energy potential, including Weibull [10], Rayleigh [11], Gamma, Lognormal [12], and more [13–15]. Among the various types of pdfs, Weibull and Rayleigh are the most widely used, mainly due to the superior performance in describing the wind speed distribution. The approach based on the different pdfs consists in assimilating the distribution law to one of these models and in determining the model parameters so that it is closest to the discrete law achieved by the statistical treatment of the wind speed measurements [16]. In the actual applications, most attention according to the wind energy assessment is given to the power output of the turbines, which is the most significant indicator for the site selection and construction. In this aspect, the proper

wind speed distribution describes the variation of the wind with respect to time and the effect of the varying wind on the power output of the turbines, according to a WT power curve. However, the seemingly good performance of wind speed distribution may not always translate to an accurate assessment of the energy potential; this indicates that the input/output relationship between the wind speed and the power output may not be accurately matched under the pdf-described wind speed information. The mismatch between wind speed and power output frequently occurs during the actual energy assessment and power generation and may result from the power output control mechanisms of the wind power generators, thus giving an inaccurate power assessment.

As is well known, the WT converts the energy of wind into electric power output at the grid connection interface, which depends on the integrated view of the complex aerodynamic, mechanic, electromagnetic, and control aspects; there is a direct connection between the wind resource and the power output. To accurately describe the characteristics of wind-related power generation and to accurately evaluate the wind energy potential, the link between the wind speed and the power produced by a wind generator is given by the so-called power curve, typically provided by the WT manufacturer. In general, a power curve describes the power delivered by a WT by representing the turbine power output as a function of the wind speed at hub height. With such a curve, the power output from a WT can be estimated without the detailed knowledge of turbine operations and its control schemes [17]. It is common that a generic equation for the modeling of the power curve will be preferred in studies on WT modeling [18–20], the analysis of wind energy potential [21], site matching [20, 22, 23], cost modeling [24], and so forth. Considering the accurate assessment of wind power potential, the influence of the WT power curve cannot be ignored [7]. According to the power output control mechanisms, the power output remains constant in the range of the rated speed to the cut-out speed, which changes the relation between the power output and the wind speed.

The power curve of a WT is obtained by the manufacturers from the field measurements of wind speed and power and partly from the environmental values (temperature, pressure, and relative humidity) [17]. The measurements are usually averaged and normalized to reference the air density using normalized procedures in predefined conditions (with flat terrain and appropriate sampling rate) [25]. When a wind farm consisting of many turbines is injected into the power grid and begins operation, the focus shifts to the entire plant's performance. An equivalent wind plant power curve becomes highly desirable and useful in predicting the plant output for a given wind forecast. In the actual power generation, the input/output relationship between the wind speed and the power output is always inconsistent with the power curve that is given to a WT, due to complex reasons such as wind direction, energy loss, local topography, and turbine layout. This makes it difficult to accurately evaluate the power potential and to provide precise estimations of the future power output; consequently, it is of great significance to enhance the performance of the equivalent power curve

modeling, and the following text focuses on this significant topic.

1.3. Original Contribution: Developed Equivalent Power Curve Modeling Strategies. The major highlight of this paper is its development of a wind power assessment based on the wind speed outputs of the numerical weather models and the developed power curve modeling methods that consider the artificial intelligence (AI) algorithm, the data quality check, and the outlier detection technique for the turbine outputs and the enhanced power curve modeling according to wind directions. Specifically, as the current generation “community” physics-based atmospheric model, the weather research and forecasting (WRF) model is now the widely used meso-scale system serving both the operational forecasting and atmospheric research needs. In this paper, the wind speed outputs from the WRF simulation are used for future power assessment; calculations indicate that the WRF-based power assessment is far more accurate than the evaluations from the basic wind speed distributions when considering the total power production of a local farm. At the first step, the single layer feed-forward neural network (SLFN) is employed for power curve modeling by learning the input/output transition through an AI-based nonlinear mapping. The SLFN is chosen mainly because of its strengths in capturing the complex nonlinear input/output relations identical to the transition from wind speed to the wind-generated power output; it enables the WRF-SLFN method to be far more effective and accurate than the original methods.

Next, two improvements based on the original WRF-SLFN are proposed to provide better assessment results. The first, named WRF-SLFN-OD, is a mixture of not only the WRF wind speed simulation and SLFN structure but also an additional data quality check and outlier detection technique. It enables the assessment process to first check and eliminate the abnormal records within the raw data set; then, the cleaned data set is regarded as the input of the original WRF-SLFN process. The second, named WRF-SLFN-WD, contains a preanalysis of the wind direction distribution and its influence on the power output, before the curve modeling process. Wind speeds are grouped into twelve directional sectors, and the most frequent wind speeds always carry the primary and most effective information of the local wind resource, considering the power potential assessment. The simulation indicates that both the WRF-SLFN-OD and WRF-SLFN-WD methods can be significant enhancements for the assessment problem.

1.4. Data Collection. To validate the effectiveness and accuracy of the proposed methods according to the wind power potential assessment problem in this paper, the available wind speed and corresponding power output records are collected from three sites in northern China (the site description is displayed in Figure 2). Specifically, both the wind speed measurements and the WRF wind speed simulations are 1-year data sets of 15-minute intervals. Each data set is randomly divided into two subsets: the training set, which accounts for 85% of the overall data, and the testing set, which is a collection of the remaining 15% of the data.

1.5. The Structure of This Paper. The rest of this paper is organized as follows. Section 2 introduces the existing works based on the historical wind speed records. Then, Section 3 presents the assessment approach combining the WRF wind simulation and turbine power curve. Two improved power curve modeling methods are proposed in Sections 4 and 5 with a case study provided in detail. Finally, Section 6 provides the conclusions.

2. Potential Assessment Based on Measured Records

This section reviews the existing works in the literature that are related to the wind power potential assessment based on the measured records of wind speed (see Figure 1).

2.1. Wind Speed Distribution of a Local Area. The analysis of the wind speed distribution at hub heights is commonly used when assessing the wind potentials at a proposed site. In the bibliography, the wind speed frequency distribution was represented by various probability density functions; the most common are Weibull, Rayleigh, Gamma, and Lognormal distributions; this paper also considers these commonly used functions.

2.1.1. Weibull Distribution of Wind Speed. The Weibull distribution is one of the most important and widely used frequency functions in the study of wind climate and wind energy [26]. The probability density function (pdf) of a two-parameter Weibull distribution can be expressed as

$$f_w(v) = \frac{k}{c} \left(\frac{v}{c}\right)^{k-1} \exp\left[-\left(\frac{v}{c}\right)^k\right], \quad v \geq 0, \quad (1)$$

where k and c are the shape parameter and scale parameter, respectively, and v represents the wind speed. The corresponding Weibull cumulative distribution function (cdf) is defined as

$$F_w(v) = 1 - \exp\left[-\left(\frac{v}{c}\right)^k\right]. \quad (2)$$

2.1.2. Rayleigh Distribution of Wind Speed. The Rayleigh distribution is another case of the Weibull distribution when setting the shape parameter as $k = 2$; experience indicates that this sufficiently represents the real wind speed distribution in certain cases [11]. The pdf of Rayleigh distribution is defined as

$$f_r(v) = \frac{v}{c^2} \exp\left(-\frac{v^2}{2c^2}\right), \quad v \geq 0, \quad (3)$$

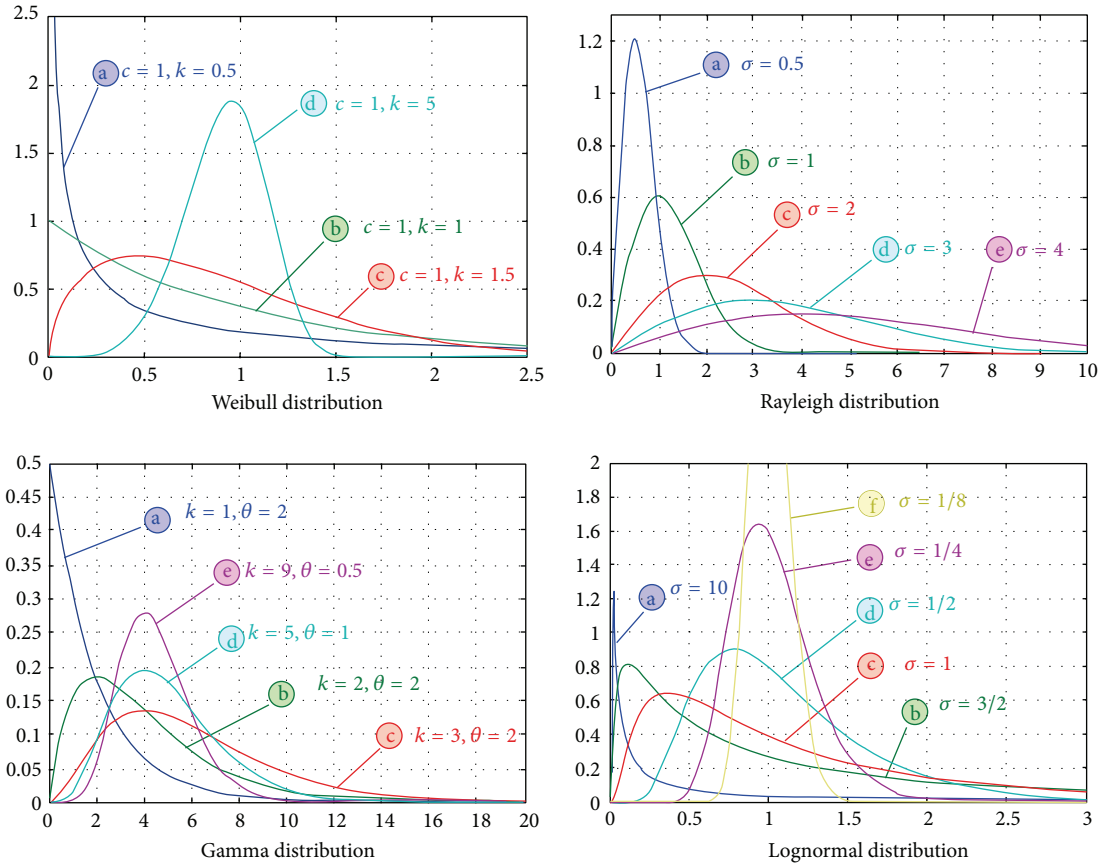


FIGURE 1: The commonly used wind speed distributions.

where c is the scale parameter and v represents the wind speed. Setting $k = 2$ in (2), the Rayleigh cdf is

$$F_r(v) = 1 - \exp\left[-\left(\frac{v}{c}\right)^2\right]. \quad (4)$$

2.1.3. Gamma Distribution of Wind Speed. The pdf of Gamma distribution is as follows:

$$f_g(v) = v^{k-1} \frac{\exp(-v/\theta)}{\Gamma(k)\theta^k}, \quad (5)$$

where k and θ are the shape and scale parameters, respectively.

2.1.4. Lognormal Distribution of Wind Speed. The pdf of Lognormal distribution is defined by

$$f_l(v) = \frac{1}{v\sigma\sqrt{2\pi}} \exp\left\{-\frac{(\ln v - \mu)^2}{2\sigma^2}\right\}, \quad (6)$$

where σ and μ are two parameters.

2.2. Fitting Result of Wind Speed Distribution. Figure 2 represents the fitting result of wind speed distribution at three stations; each of the four mentioned distributions is fitted. It

can be found that wind speed observations perform similarly between station 2 and station 3, while the data from station 1 represents a higher frequency with respect to the data interval from 5 m/s to 10 m/s. Among the different distribution functions, the Weibull pdf performs better in describing the frequency distribution of the wind speed records, according to the three selected stations in this paper. Next, the power curve is introduced to convert the wind speed into power output.

2.3. Power Curve and Statistical Power Assessment. The wind turbine is the direct transducer that delivers wind into the electric power output. The power curve is the most common representation of the relation between the wind speed and the power production, which is defined as

$$P_{wtg}(v) = \begin{cases} P_r, & v_r < v \leq v_{co}, \\ P_r \frac{v - v_{ci}}{v_r - v_{ci}}, & v_{ci} < v \leq v_r, \\ 0, & v \leq v_{ci} \text{ OR } v > v_{co}, \end{cases} \quad (7)$$

where v_{ci} , v_{co} , v_r , and P_r represent the cut-in, cut-off, rated speeds, and the rated power, respectively.

There are three key points on the power curve: (i) the cut-in speed, below which the turbine will not produce power, (ii) the rated speed, at which the rated power of the turbine

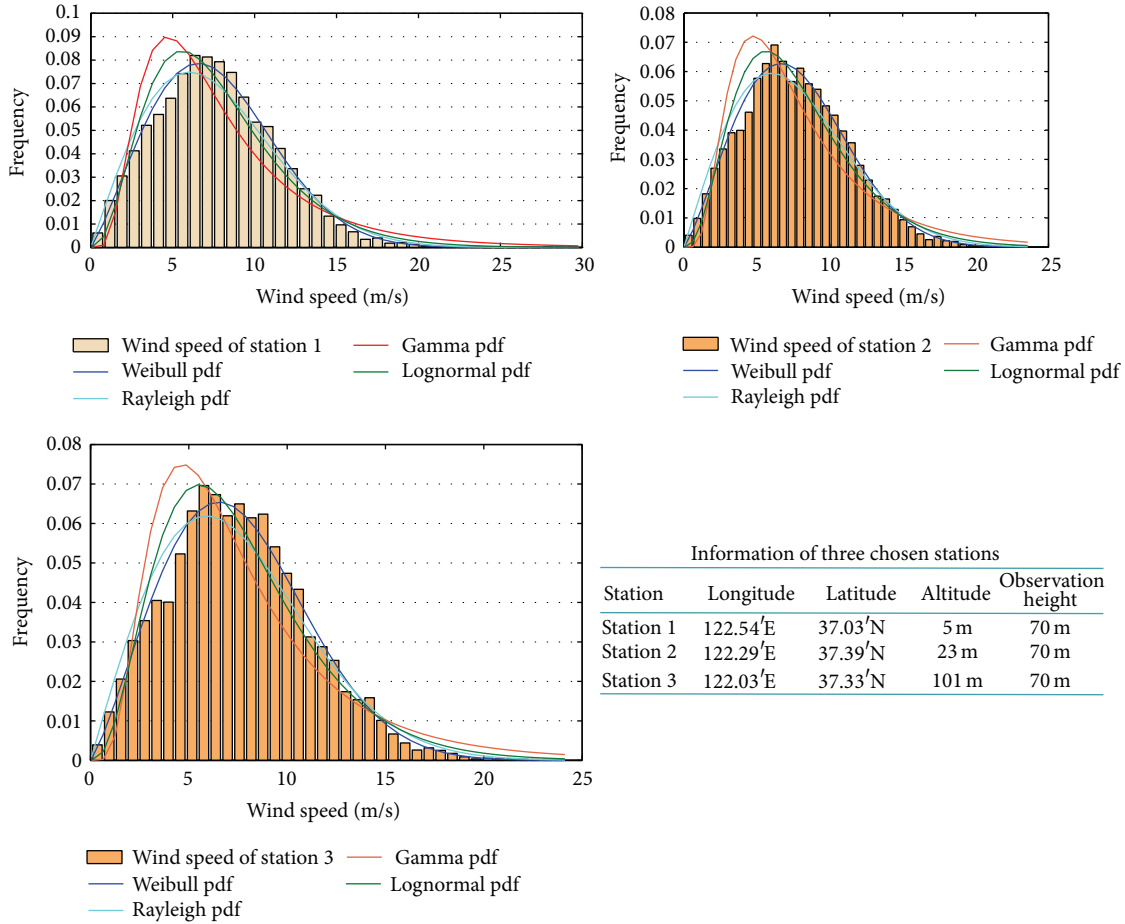


FIGURE 2: Distribution fitting according to the three stations.

is produced, and (iii) the cut-off speed, beyond which the turbine is not allowed to deliver power. Then, the power produced in a given period can be calculated by

$$E_w = T \int_0^{\infty} P_{wtg}(v) f(v) dv, \quad (8)$$

where T represents the given time and $f(v)$ is the pdf associated with the wind speed v .

3. Power Estimation with Wind Speed Outputs from the WRF Simulation

For the future potential assessment of wind-generated power output, this paper considers a combination of the atmospheric numerical simulation and the WT power curve. Specifically, the WRF model is chosen to provide a physical prediction of the future wind speed; then, the assessment of power potential can be obtained through the power curve modeling.

3.1. WRF Simulation and Model Configuration. The WRF model is now the current generation “community” physics-based atmospheric model, serving both the operational forecasting and atmospheric research needs; the WRF model has

now become one of the most popular and widely used tools for numeric weather prediction. In the WRF model, a grid is a set of three-dimensional points in space containing weather data, such as wind speed and atmospheric pressure. Each grid has a current time and an associated stop time. The WRF simulates the atmosphere using physics calculations based on the grid data and a specific physics model; then, the current time of the grid is advanced by a unit of time called a time-step [27].

In this paper, the wind speed from the WRF outputs will be used for future power assessment with the proposed power curve modeling strategies. The physical options of the WRF model are described in Table 1.

3.2. Energy Estimation and Assessment with Wind Speed Outputs from the WRF Simulation. After acquiring the wind speed outputs from the WRF simulation process, the WT power curve can be employed to transform the wind speed into power generation; thus, the future wind power potential of the chosen promising site can be obtained and can be used for further construction and operation of the wind farm.

Different from the power assessment based on the historical measurements discussed in Section 2, the developed approach here is more reasonable and effective when considering the future power potential at a local site. The reason

TABLE 1: Model configuration of the WRF simulation.

	Physical options
Cumulus parameterization	Grell 3D ensemble cumulus scheme
Short-wave radiation	RRTM scheme
Long-wave radiation	Dudhia scheme
Surface layer physics	Eta similarity
Land surface processes	Fractional sea-ice
Planetary boundary layer	Mellor-Yamada-Janjic scheme

is that the wind speed output from the WRF simulation describes the future atmospheric circumstance and conditions, which directly affect the efficiency of wind power generation and, furthermore, have an impact on the operation behavior of the wind farm. Moreover, both statistical and physical models are the popular methods to predict future wind speed; the statistical models focus more attention on finding the inner regulation of the historical data and perform better in short-term prediction. According to the assessment problem considered in this paper, physical simulation is more powerful because the input of the physical models is physical or meteorology information, such as the description of orography, roughness, obstacle, atmospheric data, and more [28]. All of these factors in actual could impact the wind speed significantly. The following sections will demonstrate that the developed assessment, combining the WRF wind speed simulation and the improved power curve modeling methods, performs decisively in the future power potential assessment according to the simulation result.

4. Equivalent Power Curve Modeling: Neural Network and Improved Methods

Power curve modeling is the most straightforward approach to accurately match the wind speed and the actual power output according to a specific condition of power generation. A single turbine power curve is determined by measuring the turbine output and inflow wind speed at the hub height. While considering the power potential assessment for a wind farm, the power curves are adversely affected by the wind farm layout and the changing environmental and topographical conditions. In fact, mainly due to the wakes created by the wind turbines upstream, the wind speed reduces the efficiency of the turbine array. Therefore, the equivalent power curve modeling is of great significance, incorporating the effect of the array efficiency, the high wind speed cut-out, the topographic effect spatial averaging, the availability, and the electrical losses [29]. Such a curve, if it can be developed, will help plant and system operators predict the plant output for a given wind speed that takes into account these pertinent factors. The following text focuses on the equivalent power curve modeling by ANNs and two improved strategies.

4.1. Basic Formulation of Single Layer Feed-Forward Neural Network (SLFN). The neural network (NN) technique is an information-processing model simulating the operation of the biological nervous system, which is widely used to model

complex functions for various applications. An NN model consists of interconnected groups of artificial neurons that emulate the function of neuron cells; therefore, it is able to identify the complicated pattern within a certain data set [30]. Considering the wind power potential assessment, it can be a significant practice to apply the NNs with other methods in modeling the relationship between the wind speed and power output.

The chosen neural network in this paper is the SLFN model, which is considered as a powerful and effective network frame to address complex problems, such as the power curve modeling problem.

Consider a set of M distinct samples $(\mathbf{x}_i, \mathbf{y}_i)$ with $\mathbf{x}_i = [x_{i1}, x_{i2}, \dots, x_{in}]^T \in \mathbb{R}^n$ and $\mathbf{y}_i = [y_{i1}, y_{i2}, \dots, y_{im}]^T \in \mathbb{R}^m$; then, a standard SLFN with N hidden neurons and activation function f is mathematically modeled as

$$\mathbf{O}_j = \sum_{i=1}^N \beta_i f_i(\mathbf{x}_j) = \sum_{i=1}^N \beta_i f(\mathbf{w}_i \mathbf{x}_j + b_i), \quad 1 \leq j \leq M, \quad (9)$$

where \mathbf{O}_j is the simulated output of SLFN, \mathbf{w}_i is the input weights connecting the i th hidden neural and the input neuron, b_i is the biases of the i th hidden neural, and β_i is the output weight vector connecting the i th hidden neural and the output neuron.

Then, the mean square error (MSE) of the SLFN simulation according to the given data can be defined as

$$E(\mathbf{w}, b, \beta) = \frac{1}{M} \sum_{j=1}^M (\mathbf{O}_j - \mathbf{y}_j)^2. \quad (10)$$

4.2. Evaluation Criteria for Modeling Accuracy. In this paper, the relative error (RE) is selected for accuracy evaluation according to the equivalent power curve modeling; the definition of RE is as follows:

$$\text{RE} = \frac{P_e - P_a}{P_a}, \quad (11)$$

where P_e and P_a are the estimated and actual power, respectively.

4.3. Power Curve Modeling Result. This section employs the SLFN to model the complex relationship between wind speed and actual power output, which is usually mismatched according to the WT power curve provided by the manufacturer. Figures 3, 4, and 5 represent the curve fitting result for each chosen station; the wind speed data used here are the WRF wind speed output, which has been introduced in Section 3.1. Generally, the larger wind speed can be transformed into higher power output; however, the transformational relation is not a simple and certain function during actual power generation due to complex reasons. A rough corresponding relation between the wind speed and the WT power output can be found, but the relationship is not very clear; the wind speeds with the same value can be transformed into different values of power output that have a large fluctuation range. As exemplified by station 1 in Figure 3,

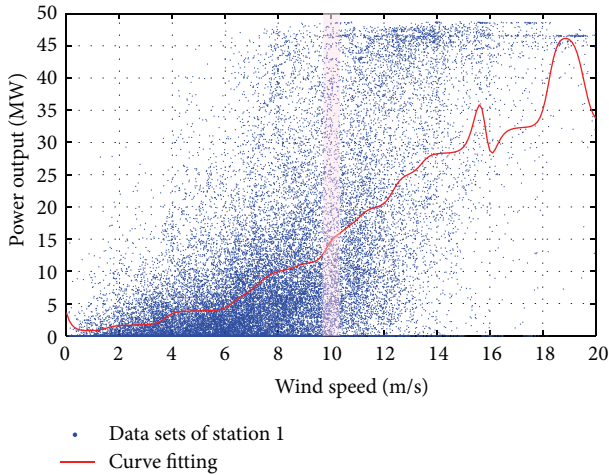


FIGURE 3: Original curve fitting result of station 1.

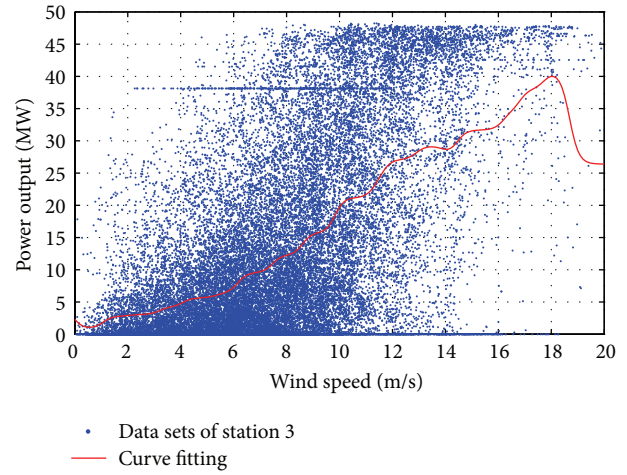


FIGURE 5: Original curve fitting result of station 3.

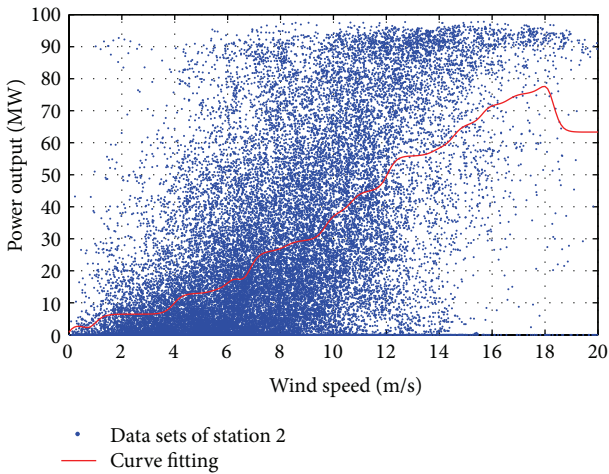


FIGURE 4: Original curve fitting result of station 2.

wind speeds of approximately 10 m/s correspond to power output ranges from 0 to approximately 50 MW. Moreover, the corresponding relation is more ruleless as the wind speed increases. This makes it quite difficult to extract the effective information of the transform relation, which is the most significant concern for an accurate power assessment.

Therefore, the SLFN is regarded as a powerful tool to learn the transition relation. It is clear that the SLFN-fitted power curve is complicated and is unlike the form of the power curve provided by the manufacturer. When the wind speed value is relatively small, the SLFN-fitted power curve exhibits a steady upward trend as the wind speed increases. For the larger wind speeds, the fitting result is complex and is obviously somewhat lower than the normal power outputs. This may result from the abnormal outputs that existed in the data sets, which have a large wind speed but quite low power output; a detailed discussion about abnormal outputs will be provided in the next section.

Traditional power assessment is usually based on the frequency distribution of the wind speed, and it then transforms the wind speed into the power output. A significant undertaking is to compare the performance among the developed WRF-SLFN method with the methods according to a certain pdf of the wind speed. Figure 6 provides a comparison of the results; the testing data are randomly selected from the entire data set with a proportion of 15% introduced in Section 1.4. The results indicate that the strength of the WRF-SLFN method may be its overall grasp when considering a power assessment problem; these results can also be found in Table 2. Divide the range of power output into ten intervals as exhibited in Figure 6; clearly, the power output has a high frequency according to the first subinterval that contains the power outputs with the smallest values. Each of the five methods mismatches this characteristic. Specifically, the methods that depend on the Weibull and Rayleigh distributions perform similarly to each other; they also have similar RE values. The Lognormal-SLFN method exhibits a large assessment error in each of the three stations, while the Gamma-SLFN obtains a relatively lower RE. Meanwhile, the WRF-SLFN method performs better; the frequency of the estimated power output steadily decreases with the rise of the power output values. It has a good ability for power assessment, especially for the intervals with larger wind speeds. Comparing the RE values of the different methods, the WRF-SLFN obtains the lowest RE value in stations 1 and 2 and has the same error as the Weibull-SLFN in station 3. In the following text, the original WRF-SLFN method can be improved to provide a more accurate assessment of the wind power potential.

5. Improvement according to a Data Quality Check and Outlier Detection Technique

The WRF-SLFN approach performs much better compared with the other four pdf-SLFN methods, which was introduced in the above text; the developed method also has its weakness, mainly due to the use of unfiltered raw data sets.

TABLE 2: Performance comparison between the WRF-SLFN and the four pdf-SLFN methods.

		RE of wind power assessment					
		0–10 MW	10–20 MW	20–30 MW	30–40 MW	40–50 MW	Total
Site 1	Weibull-SLFN	0.22	0.35	0.73	1.06	-0.41	-0.28
	Rayleigh-SLFN	0.38	0.71	0.75	0.61	-0.66	-0.23
	Gamma-SLFN	0.54	0.49	0.46	0.32	-0.53	-0.15
	Lognormal-SLFN	0.04	0.66	1.51	1.36	-0.19	-0.56
	WRF-SLFN	0.40	0.99	0.56	0.05	-0.86	-0.09
		0–20 MW	20–40 MW	40–60 MW	60–80 MW	80–100 MW	Total
Site 2	Weibull-SLFN	0.40	0.50	0.32	1.27	-1.00	-0.19
	Rayleigh-SLFN	0.40	0.81	0.59	0.71	-1.00	-0.19
	Gamma-SLFN	0.71	0.65	0.23	0.41	-0.70	-0.14
	Lognormal-SLFN	0.13	0.70	0.86	1.30	-0.81	-0.37
	WRF-SLFN	0.44	1.07	0.46	-0.03	-0.85	-0.10
		0–10 MW	10–20 MW	20–30 MW	30–40 MW	40–50 MW	Total
Site 3	Weibull-SLFN	0.62	0.34	1.15	0.99	-1.00	-0.20
	Rayleigh-SLFN	0.72	0.63	1.40	0.42	-1.00	-0.18
	Gamma-SLFN	0.77	0.54	1.29	0.37	-1.00	-0.14
	Lognormal-SLFN	0.29	0.56	2.10	1.07	-0.89	-0.40
	WRF-SLFN	0.76	1.02	0.60	0.57	-0.85	-0.20

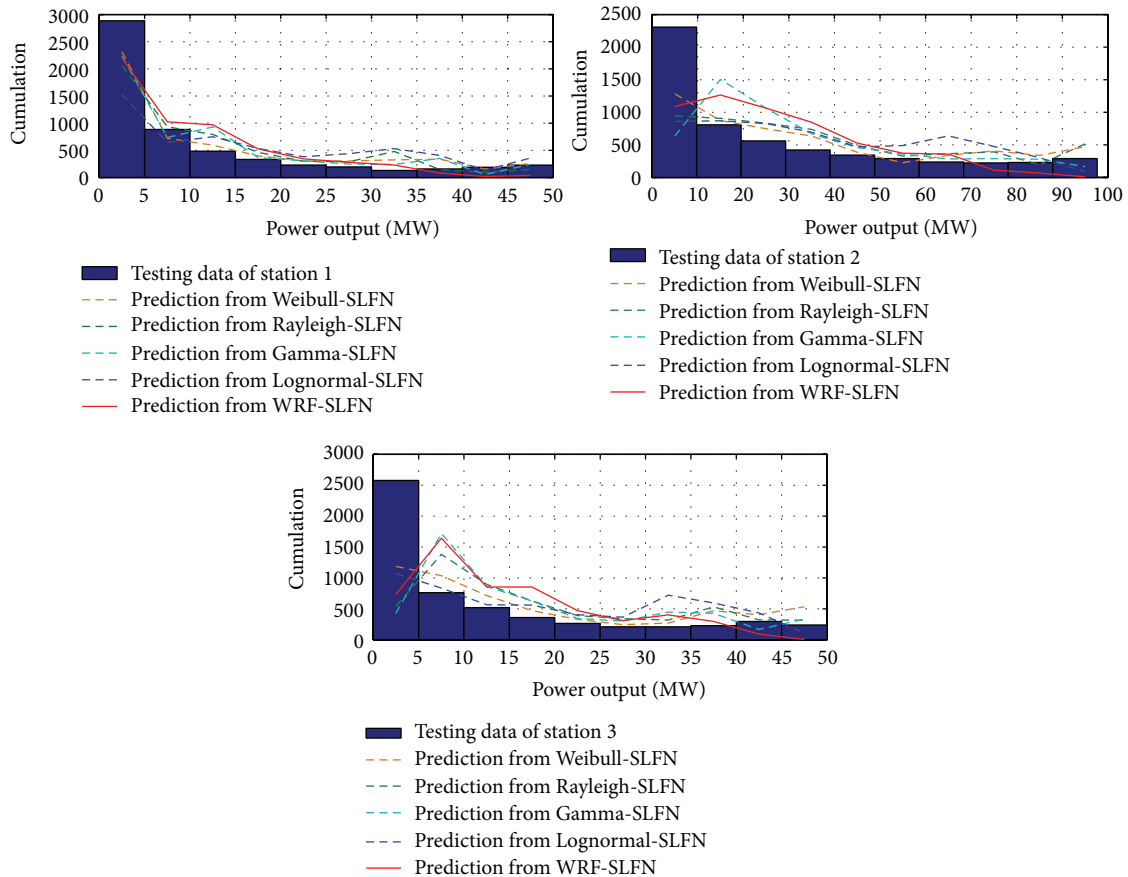


FIGURE 6: Comparison between the WRF-SLFN and the assessments based on wind speed distributions.

5.1. Outlier within Measurements. It is clear that the wind plant power curve may have a general shape that is similar to the power curve of a single turbine. Figures 3–5 demonstrate that the SLFN-fitted power curve is obviously lower than the expected form; this may be the result of the abnormal values of the power output within the raw data sets. Considering the power curve modeling for a wind farm, the abnormal value indicates that the actual power output contains serious energy loss, as Figure 7 illustrates. Furthermore, the abnormal power output leads the fitted power curve far from the ideal curve, and the gap between the curves becomes larger with the increase in the wind speed. In addition, from the scatter plot, it can be found that the raw data set needs additional cleaning to eliminate the apparent outliers. Therefore, a data quality check and outlier detection process is necessary to eliminate the obvious data errors, such as abnormal output, constant value, and negative values, and to provide a more effective result for the wind power curve modeling.

5.2. Data Quality Check and Outlier Detection Technique. The data quality check and outlier detection technique adopted in this paper was introduced in [31], initially used for the power loss calculation. Set the original data sets as (x_i, y_i) , $i = 1, 2, \dots, n$; then the WT active output curve $f(x)$ can be expressed as a k -order polynomial function of x :

$$f(x_i, \beta) = \sum_{j=0}^k \beta_j x_i^j. \quad (12)$$

Define the signal residual, which represents the deviation between the observed and ideal power outputs, as follows:

$$r_i = (y_i - f(x_i, \beta))^2. \quad (13)$$

Thus, the total signal residual is

$$S = \sum_{i=1}^n r_i = \sum_{i=1}^n (y_i - f(x_i, \beta))^2. \quad (14)$$

The key concept of this method is to find an optimal β , which makes the observation sets in accordance with (13) through an iterative regression process. Define an index

$$K = \sum_{j=0}^k \beta_j^2. \quad (15)$$

The value of K will tend to be stable when the estimation of the WT output approximates to the ideal output. Then, the termination condition of iteration is

$$\Delta K = K_{p+1} - K_p < \xi, \quad (16)$$

where K_p represents the value of K with respect to the p th iteration and ξ is a threshold value.

5.3. Improved Power Curve Modeling with Outlier Eliminated. During the power curve modeling process addressed by the WRF-SLFN method, it is demonstrated that using the entire

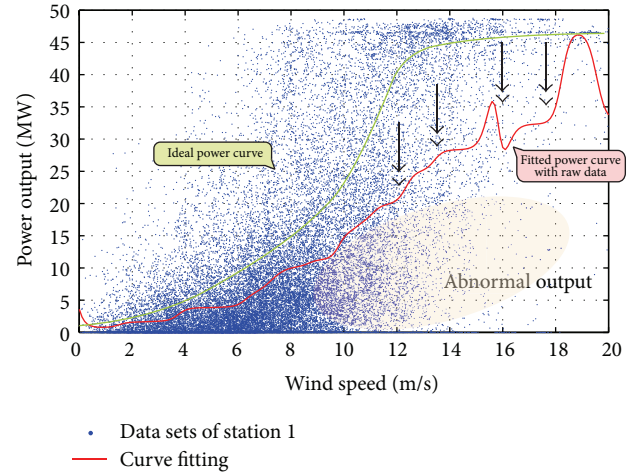


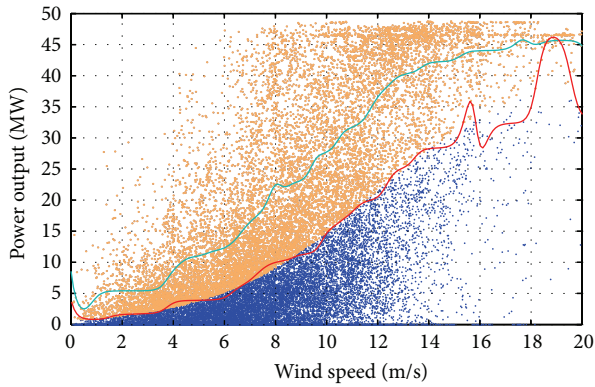
FIGURE 7: Abnormal power output within the raw data sets.

data sets is not necessary and will not improve the model performance. As a consequence, this section displays the power curve modeling result by using an improved methodology that combines the SLFN with the outlier detection technique; this improved power curve modeling method is named the SLFN-OD. During the SLFN-OD process, the data quality check and outlier detection technique introduced in Section 5.2 is adopted as the first step to determine the abnormal values within the raw data set. After that, the detected abnormal subset is eliminated from the raw data set, and the cleaned data set is chosen as an input of the SLFN structure. Figures 8, 9, and 10 represent the curve fitting results of both the cleaned and raw data sets at all three stations selected in this paper. In the main, the power curve fitted by the cleaned data sets is above the curve that is modeled with the raw data set; the gap between the two power curves expands with the increase of wind speed. This process will enhance the performance of the power curve modeling, especially for the subintervals with large wind speeds. It can be regarded as a direct benefit from the detection and elimination process of the outliers that are contained in the raw data sets.

Table 3 provides the performance comparison between the WRF-SLFN and the improved WRF-SLFN-OD methods. Similar to the discussion in Section 4.3, here, the range of power output is also divided into five subintervals for each of the three stations. In the gross, the improved WRF-SLFN-OD method outperforms the WRF-SLFN with an effective enhancement according to the RE calculation; it leads to a RE reduction of 22.22%, 30.00%, and 70.00% according to the three stations, respectively, compared with the WRF-SLFN method. This indicates that the WRF-SLFN-OD brings a mean RE reduction of 40.74% compared to the original RE. Specifically, in the first subinterval for all three stations, the WRF-SLFN-OD provides an apparently higher assessment than the actual power output; this results in the negative RE values according to these subintervals. While considering the other subintervals, the WRF-SLFN-OD brings significant improvements in most cases, especially in the second and

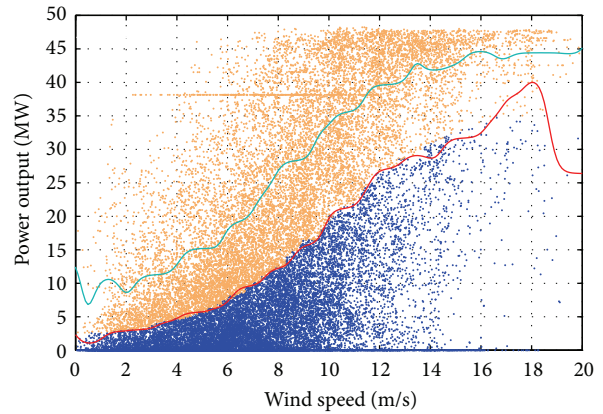
TABLE 3: Performance comparison between the WRF-SLFN and WRF-SLFN-OD methods.

		RE of wind power assessment					
		0–10 MW	10–20 MW	20–30 MW	30–40 MW	40–50 MW	Total
Site 1	WRF-SLFN	0.40	0.99	0.56	0.05	-0.86	-0.09
	WRF-SLFN-OD	-0.48	0.24	0.41	0.01	-0.01	-0.07
		0–20 MW	20–40 MW	40–60 MW	60–80 MW	80–100 MW	Total
Site 2	WRF-SLFN	0.44	1.07	0.46	-0.03	-0.85	-0.10
	WRF-SLFN-OD	-1.00	-0.83	-0.21	0.31	0.11	-0.07
		0–10 MW	10–20 MW	20–30 MW	30–40 MW	40–50 MW	Total
Site 3	WRF-SLFN	0.76	1.02	0.60	0.57	-0.85	-0.20
	WRF-SLFN-OD	-0.61	0.28	0.45	0.12	-0.15	-0.06



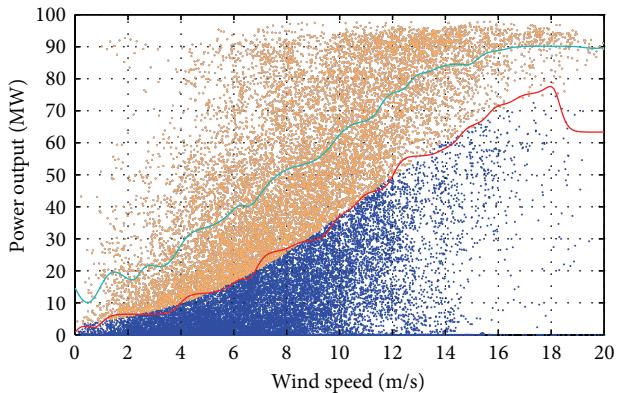
• Raw data of station 1 — Curve fitting using raw data
 • Cleaned data of station 1 — Curve fitting using cleaned data

FIGURE 8: Curve fitting using the cleaned data from station 1.



• Raw data of station 3 — Curve fitting using raw data
 • Cleaned data of station 3 — Curve fitting using cleaned data

FIGURE 10: Curve fitting using the cleaned data from station 3.



• Raw data of station 2 — Curve fitting using raw data
 • Cleaned data of station 2 — Curve fitting using cleaned data

FIGURE 9: Curve fitting using the cleaned data from station 2.

last subintervals. This enables the improved WRF-SLFN-OD method to construct a more proper model of the power curve fitting and to provide a more accurate assessment of the wind power output.

6. Improvement Considering Wind Direction Modeling

During the abovementioned modeling processes, discussions on wind speed only focused on the numerical value; however, there is another important characteristic, wind direction, which will be quite helpful in wind-related modeling such as the wind power assessment discussed in this paper.

6.1. Performance and Analysis according to Wind Direction.

Considering a specific local site, wind direction has its distinctive distribution and characteristic. Exemplified by the data collected from station 1, Figure 11 represents the distribution of the wind direction through a wind rose map. Specifically, the wind speed observations are grouped into twelve directional sectors, as the wind rose map indicates; the east direction is set as zero degree, and each sector contains a range of thirteen degrees. For station 1, the prevailing wind direction during the period when the data are available is between 330° and 360°; the wind blows from this sector more than 15% of the time. Moreover, the most frequent wind directions of stations 2 and 3 are also located in the last directional sector, the same as in station 1; the wind rose maps of these two stations are displayed in Figure 13.

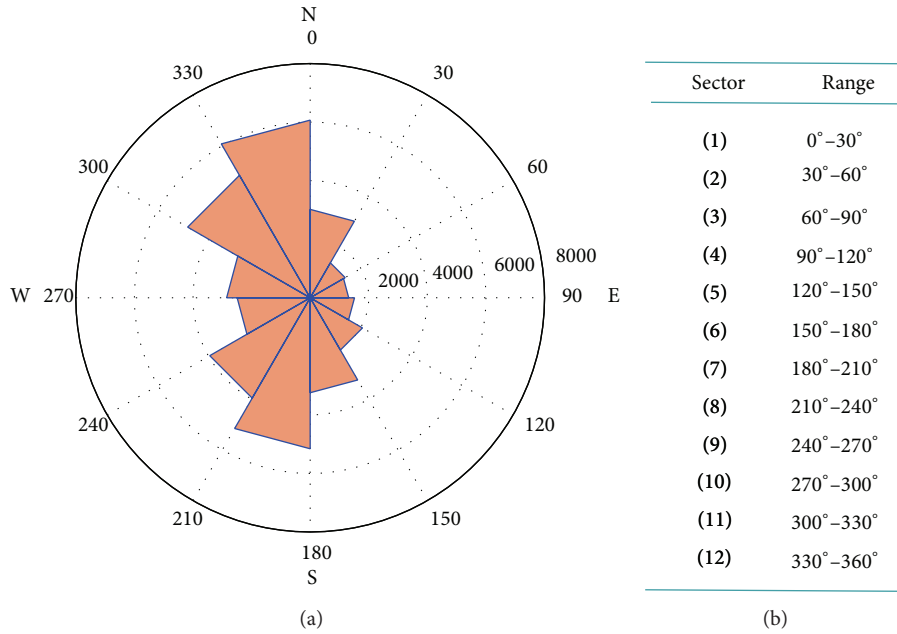


FIGURE 11: Wind rose of station 1 and the division of the wind direction.

The layout of turbines at a wind farm is always designed to take advantage of the prevailing wind directions because the wind from other directions may not produce as much power as the wind from the prevailing direction as a result of the wake effect. Thus, what is the relationship between the directional wind speed and the actual power output? Figure 12 exhibits the power output performance according to the different wind direction sectors, also exemplified by station 1; the numbers of wind speed sectors accord with the division exhibited in Figure 11. It is clear that the transformation relation varies according to the wind speed from the different directional sectors. The most important reason may be that the WTs are not always arrayed in conformity with the direction of the wind due to the change of the wind direction. Although the yaw device can make an adjustment to the WT heading, depending on the anemometer and wind vane at the hub height, some lag cannot be eliminated. As a consequence, the wind speeds that come from the prevailing direction can be transformed into power outputs with the maximum utilization rate. This indicates that the most frequent wind speeds carry the major information of the local wind, considering the wind power generation from the WTs; the winds from other directional sectors, especially the positions that are nearly perpendicular to the prevailing direction, may not be helpful in improving the model performance and may introduce additional errors during the wind-related modeling process.

6.2. Improved Power Curve Modeling Considering Wind Direction. The above discussion indicates that the wind farm production varies under the different wind directions; the wind direction is also a significant factor for an accurate estimation of the wind power output. This section develops an improved FLFN-handled power curve modeling with the wind direction factor; it is designated the SLFN-WD. Figures

14, 15, and 16 display the curve fitting results using the data in the prevailing directional sector and using the raw data for each of the three selected stations. On the whole, the power curves fitted by the prevailing directional data sets exhibit the same trend as the curves modeled by the raw data sets, for each station. This indicates that the wind speeds located in the most frequent directional sector contain the major and most effective information of the local wind resource because the prevailing directional wind speed has the highest cumulative frequency and the most power potential. In addition, there are differences between the curves modeled using the prevailing direction and raw data sets. Power curves fitted with the prevailing directional wind speeds are overall above those fitted by the raw sets; the gap between these two categories becomes larger with the increase of the wind speed value.

The performance of the WRF-SLFN-WD is represented in Figure 17; both the polar diagrams and a table of the RE comparison are included. The result demonstrates that the power curve modeling process performs well in the prevailing directional sector; it achieves a quite low RE in all three stations. At the same time, the power curve modeling in certain directional sectors leads to a large evaluation error, even higher than 1.50. Therefore, the power curve modeling with the unselected raw data may introduce additional interferences instead of leading to an error reduction; modeling with the prevailing directional wind speeds is useful for obtaining the effective information of the power transformation and for providing an accurate assessment of the local wind power potential.

7. Conclusion

To build up wind farms, it is essential to perform an accurate assessment of the wind energy potential at the promising

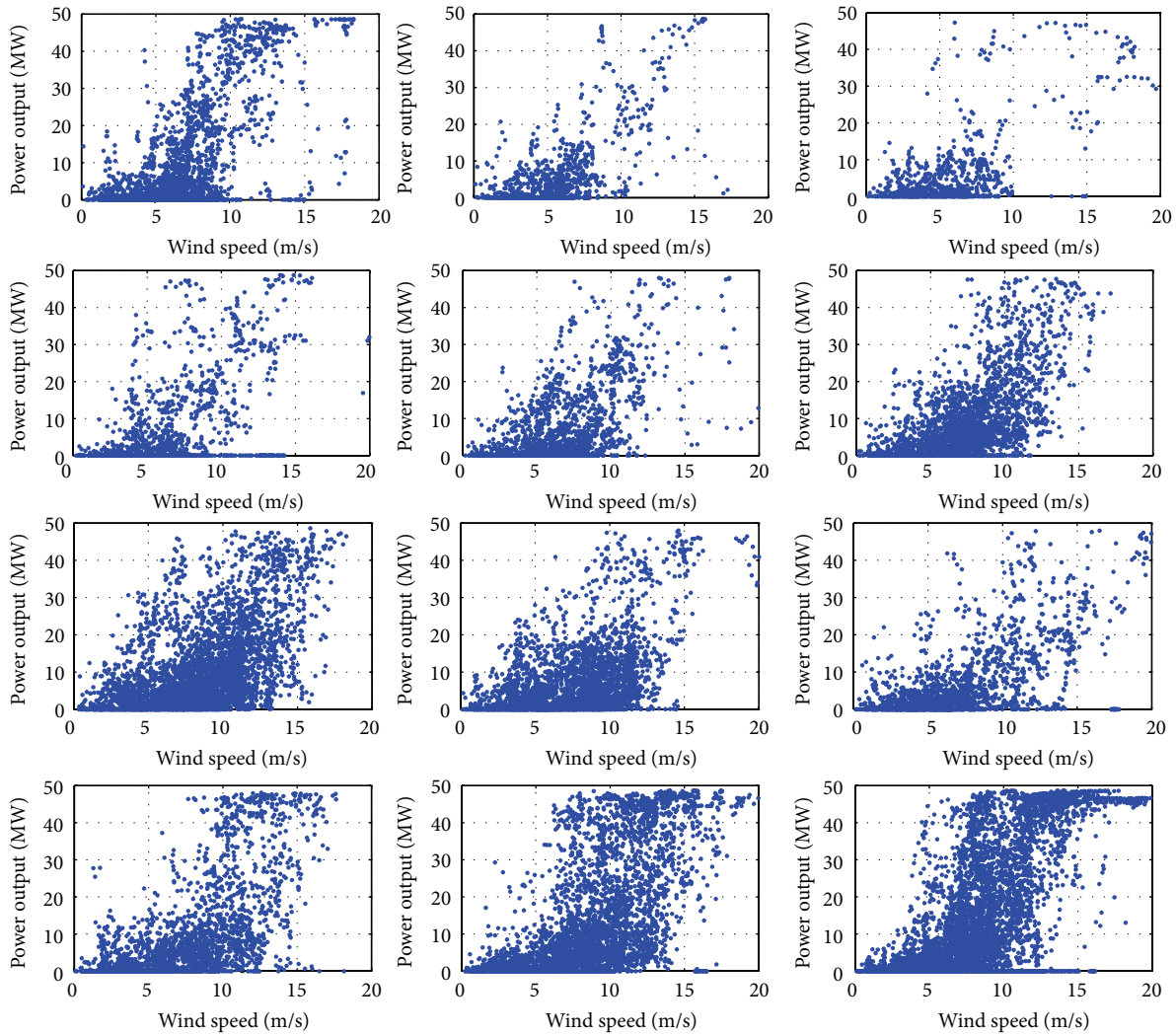


FIGURE 12: Power output performance according to the different wind direction sectors, exemplified by station 1.

sites because it is a necessary and crucial step both in the preevaluation for the site selection and in the further planning of the project. As one of the most important factors during the assessment process, the knowledge of wind power transformation, from the wind speed to the wind-generated power output, is required, but it is not an easy task. The statistical analysis, concerning the use of the various pdfs to describe the wind speed frequency distributions, is generally used. However, their performance is expected to be enhanced in the actual applications.

This original method of wind power assessment is a combination of the WRF wind speed simulation and the SLFN algorithm, due to the recognized strengths of both methods. In most cases, the WRF-SLFN method demonstrates good performance compared with the pdf-based power assessment. Next, two improvements are proposed through the aid of the abovementioned data quality check and the outlier detection technique and the directional power curve

modeling method, named the WRF-SLFN-OD and the WRF-SLFN-WD. Specifically, the first improved method contains a data filtering process that eliminates the abnormal outputs within the raw data set and uses the cleaned set as the input of the original SLFN-fitting structure. The WRF-SLFN-OD method leads to an RE reduction of 40.74%, which is the mean value from the simulation of all three stations compared with the original RE. Then, the WRF-SLFN-WD method includes a data analysis according to the twelve directional sectors of the local wind speeds; the data with the prevailing directional wind speeds is chosen for further power curve modeling and power potential assessment. The result indicates that power curve modeling with unselected raw data may introduce additional interferences instead of leading to an error reduction; thus, both of the proposed methods are of great significance to filter the effective information of the power transformation and to provide an accurate assessment of the local wind power potential.

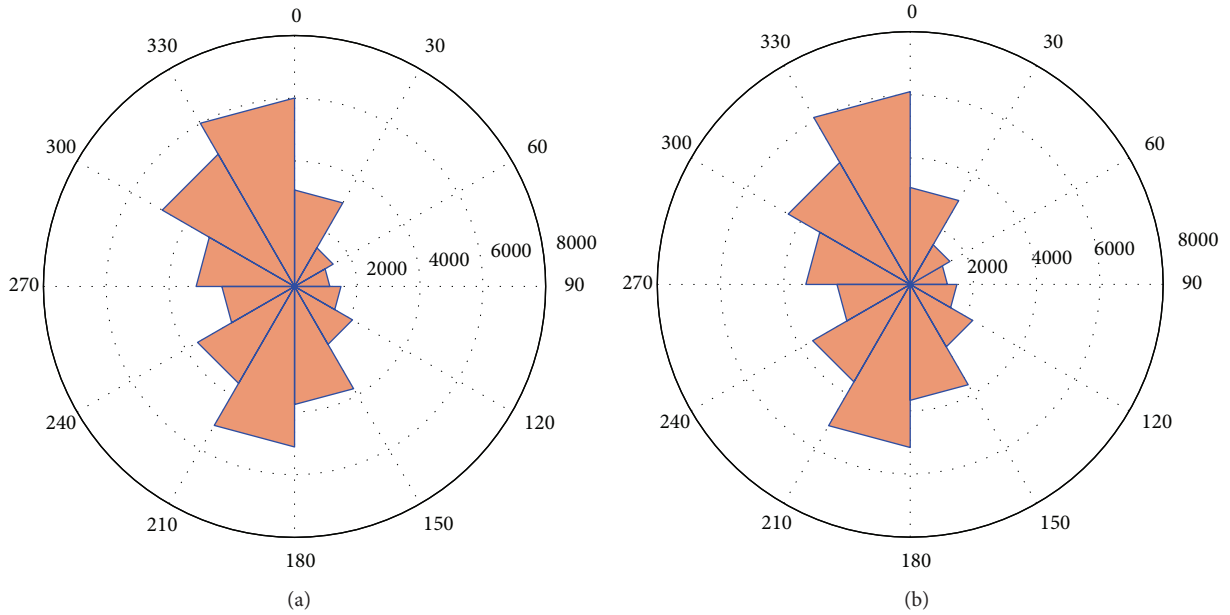


FIGURE 13: Wind rose of stations 2 and 3.

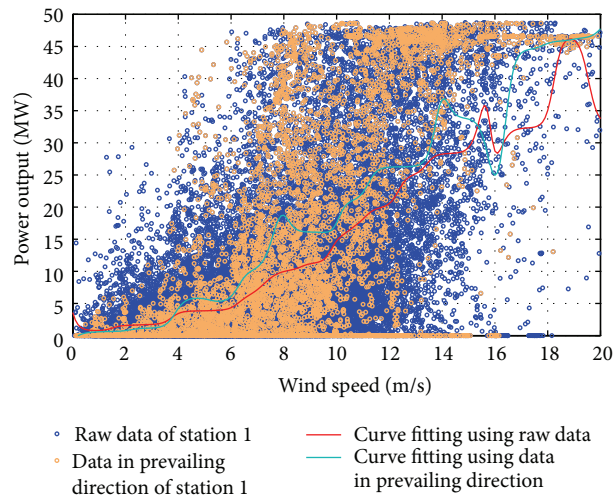


FIGURE 14: Curve fitting using the data in the prevailing direction of station 1.

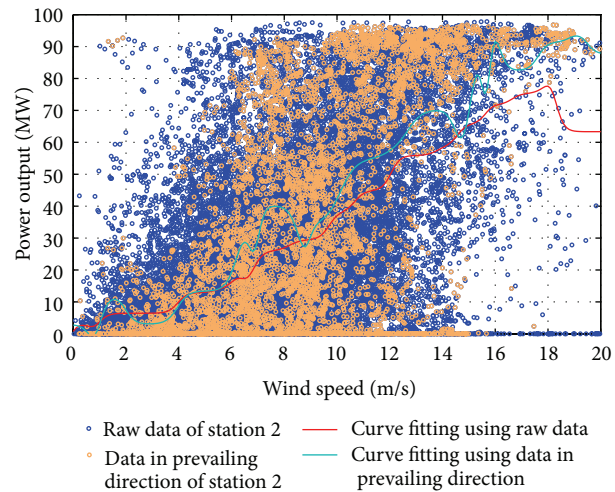


FIGURE 15: Curve fitting using the data in the prevailing direction of station 2.

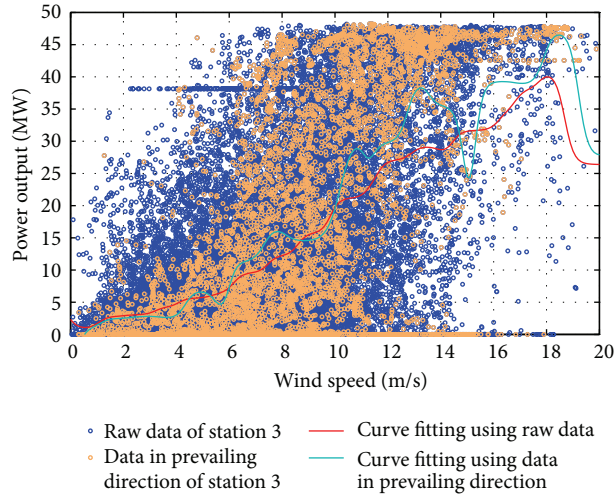


FIGURE 16: Curve fitting using the data in the prevailing direction of station 3.

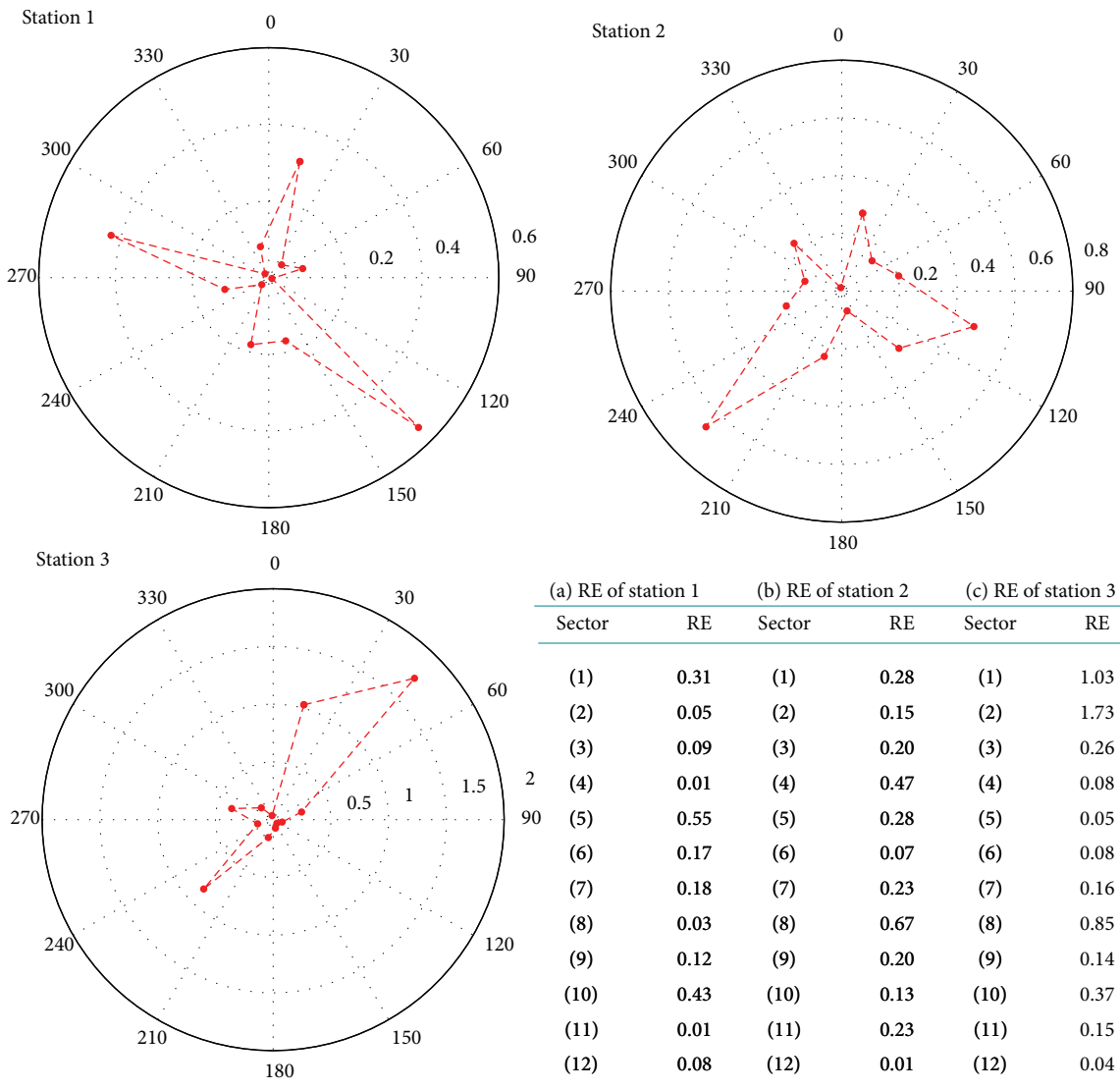


FIGURE 17: Performance of power curve modeling considering the wind direction.

Conflict of Interests

The authors declare that there is no conflict of interests regarding the publication of this paper.

Acknowledgment

This work was supported by CAS Strategic Priority Research Program Grant no. XDA05110305.

References

- [1] I. Fyrippis, P. J. Axaopoulos, and G. Panayiotou, "Wind energy potential assessment in Naxos Island, Greece," *Applied Energy*, vol. 87, no. 2, pp. 577–586, 2010.
- [2] K. Radics and J. Bartholy, "Estimating and modelling the wind resource of Hungary," *Renewable and Sustainable Energy Reviews*, vol. 12, no. 3, pp. 874–882, 2008.
- [3] A. Ucar and F. Balo, "Investigation of wind characteristics and assessment of wind-generation potentiality in Uludag-Bursa, Turkey," *Applied Energy*, vol. 86, no. 3, pp. 333–339, 2009.
- [4] S. Salcedo-Sanz, Á. M. Pérez-Bellido, E. G. Ortiz-García, A. Portilla-Figueras, L. Prieto, and F. Correoso, "Accurate short-term wind speed prediction by exploiting diversity in input data using banks of artificial neural networks," *Neurocomputing*, vol. 72, no. 4–6, pp. 1336–1341, 2009.
- [5] G. Xydis, C. Koroneos, and M. Loizidou, "Exergy analysis in a wind speed prognostic model as a wind farm siting selection tool: a case study in Southern Greece," *Applied Energy*, vol. 86, no. 11, pp. 2411–2420, 2009.
- [6] Y. Zhou, W. X. Wu, and G. X. Liu, "Assessment of onshore wind energy resource and wind-generated electricity potential in Jiangsu, China," *Energy Procedia*, vol. 5, pp. 418–422, 2011.
- [7] K. Chen, M. X. Song, and X. Zhang, "A statistical method to merge wind cases for wind power assessment of wind farm," *Journal of Wind Engineering and Industrial Aerodynamics*, vol. 119, pp. 69–77, 2013.
- [8] S. A. Grady, M. Y. Hussaini, and M. M. Abdullah, "Placement of wind turbines using genetic algorithms," *Renewable Energy*, vol. 30, no. 2, pp. 259–270, 2005.
- [9] C. Stathopoulos, A. Kaperoni, G. Galanis, and G. Kallos, "Wind power prediction based on numerical and statistical models," *Journal of Wind Engineering and Industrial Aerodynamics*, vol. 112, pp. 25–38, 2013.
- [10] R. Tchinda and E. Kaptouom, "Wind energy in Adamaoua and North Cameroon provinces," *Energy Conversion and Management*, vol. 44, no. 6, pp. 845–857, 2003.
- [11] S. Mathew, K. P. Pandey, and A. Kumar, "Analysis of wind regimes for energy estimation," *Renewable Energy*, vol. 25, no. 3, pp. 381–399, 2002.
- [12] R. E. Luna and H. W. Church, "Estimation of long-term concentration using a universal wind speed distribution," *Journal of Applied Meteorology and Climatology*, vol. 13, no. 8, pp. 910–916, 1974.
- [13] J. Zhou, E. Erdem, G. Li, and J. Shi, "Comprehensive evaluation of wind speed distribution models: a case study for North Dakota sites," *Energy Conversion and Management*, vol. 51, no. 7, pp. 1449–1458, 2010.
- [14] P. Ramírez and J. A. Carta, "The use of wind probability distributions derived from the maximum entropy principle in the analysis of wind energy. A case study," *Energy Conversion and Management*, vol. 47, no. 15–16, pp. 2564–2577, 2006.
- [15] S. Akpinar and E. K. Akpinar, "Estimation of wind energy potential using finite mixture distribution models," *Energy Conversion and Management*, vol. 50, no. 4, pp. 877–884, 2009.
- [16] L. Thiaw, G. Sow, S. S. Fall, M. Kasse, E. Sylla, and S. Thioue, "A neural network based approach for wind resource and wind generators production assessment," *Applied Energy*, vol. 87, no. 5, pp. 1744–1748, 2010.
- [17] C. Carrillo, A. F. Obando Montaña, J. Cidrás, and E. Díaz-Dorado, "Review of power curve modelling for wind turbines," *Renewable and Sustainable Energy Reviews*, vol. 21, pp. 572–581, 2013.
- [18] V. Thapar, G. Agnihotri, and V. K. Sethi, "Critical analysis of methods for mathematical modelling of wind turbines," *Renewable Energy*, vol. 36, no. 11, pp. 3166–3177, 2011.
- [19] C. Carrillo, A. Feijóo, and J. Cidrás, "Comparative study of flywheel systems in an isolated wind plant," *Renewable Energy*, vol. 34, no. 3, pp. 890–898, 2009.
- [20] S. H. Jangamshetti and V. Guruprasada Rau, "Normalized power curves as a tool for identification of optimum wind turbine generator parameters," *IEEE Transactions on Energy Conversion*, vol. 16, no. 3, pp. 283–288, 2001.
- [21] F. A. L. Jowder, "Wind power analysis and site matching of wind turbine generators in Kingdom of Bahrain," *Applied Energy*, vol. 86, no. 4, pp. 538–545, 2009.
- [22] S.-Y. Hu and J.-H. Cheng, "Performance evaluation of pairing between sites and wind turbines," *Renewable Energy*, vol. 32, no. 11, pp. 1934–1947, 2007.
- [23] M. EL-Shimy, "Optimal site matching of wind turbine generator: case study of the Gulf of Suez region in Egypt," *Renewable Energy*, vol. 35, no. 8, pp. 1870–1878, 2010.
- [24] R. Chedid, H. Akiki, and S. Rahman, "A decision support technique for the design of hybrid solar-wind power systems," *IEEE Transactions on Energy Conversion*, vol. 13, no. 1, pp. 76–83, 1998.
- [25] F. Spertino, P. Di Leo, I. Ilie, and G. Chicco, "DFIG equivalent circuit and mismatch assessment between manufacturer and experimental power-wind speed curves," *Renewable Energy*, vol. 48, pp. 333–343, 2012.
- [26] T. Maatallah, S. E. Alimi, A. W. Dahmouni, and S. B. Nasrallah, "Wind power assessment and evaluation of electricity generation in the Gulf of Tunis, Tunisia," *Sustainable Cities and Society*, vol. 6, no. 1, pp. 1–10, 2013.
- [27] S. M. Sadjadi, "Weather research and forecasting model 2.2 documentation: a step-by-step guide of a model run," Tech. Rep. FIU-SCIS-2007-09-02, 2007.
- [28] L. Landberg, "Short-term prediction of the power production from wind farms," *Journal of Wind Engineering and Industrial Aerodynamics*, vol. 80, no. 1–2, pp. 207–220, 1999.
- [29] M. Lydia, S. S. Kumar, A. I. Selvakumar, and G. E. Prem Kumar, "A comprehensive review on wind turbine power curve modeling techniques," *Renewable and Sustainable Energy Reviews*, vol. 30, pp. 452–460, 2014.
- [30] S. Haykin, *Neural Networks; A Comprehensive Foundation*, Prentice Hall, New Jersey, NJ, USA, 1999.
- [31] Z. Xiaodan and J. N. Jiang, "Estimation of loss of wind energy in large-scale wind farm," *Automation of Electric Power Systems*, vol. 12, article 020, 2009.